LIBRARY
ROYAL AIRCRAFT ESTABLISHMENT
BEDFORD.

R. & M. No. 3036
(18,474)
A.R.C. Technical Report

MINISTRY OF SUPPLY

AERONAUTICAL RESEARCH COUNCIL
REPORTS AND MEMORANDA

A Method for Calculating the Pressure Distribution over Jet-Flapped Wings

By

D. KÜCHEMANN

Crown Copyright Reserved

LONDON: HER MAJESTY'S STATIONERY OFFICE
1957
PRICE 7*s.* 6*d.* NET

A Method for Calculating the Pressure Distribution over Jet-Flapped Wings

By

D. KÜCHEMANN

COMMUNICATED BY THE DIRECTOR-GENERAL OF SCIENTIFIC RESEARCH (AIR), MINISTRY OF SUPPLY

Reports and Memoranda No. 3036*

May, 1956

Summary.—The incompressible flow past an aerofoil with a thin jet emerging from its lower surface somewhere near the trailing edge is considered. Based on unpublished work of Gates, Maskell and Spence, a simple method is described for calculating the pressure distribution over wings of non-zero thickness. The effects of finite aspect ratio and of camber are included and the method can be used for design purposes. The possible effects of sweep are briefly discussed. It is pointed out that a saddleback chordwise loading is typical for aerofoils with jets and that this is the basic reason for many of the aerodynamic advantages of the jet-flap system.

1. *Introduction.*—The ' jet-flap ' system, as recently described by Davidson[1], has been treated in its physical aspects by Maskell and Gates (unpublished); and thin-aerofoil theory has been applied by D. A. Spence[2] to calculate the circulation and the chordwise loading for a thin flat aerofoil with a thin shallow jet emerging from the trailing edge. The latter results can be used to devise a simplified method for calculating the pressure distribution, if the external lift force and the jet momentum are known. Such an extension of the existing method is worthwhile if the effects of non-zero thickness and of camber can be included and if it can readily be extended to wings of finite aspect ratio and to swept wings. Further, the method should be simple enough to serve as a basis for a rational jet-flap wing design. It is the aim of the present paper to describe such a method, which incorporates the jet flap as a special case in the general aerofoil theory of Refs. 4 and 8.

The considerations in this note are restricted to incompressible and inviscid flow although some viscosity effects are briefly mentioned. Further, only the forces on the external surfaces of the aerofoil are considered. This leaves out the flow phenomena near the exit nozzle as well as all the problems connected with the propulsive efficiency of the system and the integration of the lift and propulsion units. In particular, internal forces and energy losses are not considered (for these *see*, for example, Ref. 9). Questions concerning the stability and control of such aerofoils are also ignored.

2. *Lift and Drag Forces on a Wing at Zero Incidence without Jet.*—As a preliminary study, consider the problems of how a lift force can be produced by a wing at zero angle of incidence and how the induced drag can be accommodated. The circulation associated with the lift force must differ from the Kutta value (which is zero) and it must be such that the rear stagnation point is displaced forward from the trailing edge by the same amount as the front stagnation point is displaced downstream from the leading edge. This may be considered as a special case of the ' Thwaites flap[3] '.

* R.A.E. Report Aero. 2573, received 2nd June, 1956.

We realise that, by dropping the Kutta condition, the solution for the chordwise loading of a flat wing of infinite span is no longer unique. The solution $l(x)$ with $x = 0$ at the leading edge and $x = 1$ at the trailing edge, of the downwash equation:

$$\frac{1}{\pi}\int_0^1 l(x')\,\frac{dx'}{x - x'} = 0$$

now takes the general form:

$$l(x) = \text{const}\left\{\left(\frac{1-x}{x}\right)^{1/2} + \left(\frac{x}{1-x}\right)^{1/2}\right\},$$

whereas the second term on the right-hand side of the last equation vanishes if the Kutta condition $l(+1) = 0$ is applied.

For a flat wing of infinite span, the chordwise loading for a given lift force can be seen at once as being the sum of two ' flat-plate ' distributions, as in Fig. 1, each of them being a solution for the flat plate at incidence. Whereas $l_1(x)$ produces a uniform downwash, $\alpha_{e1} = C_{L1}/2\pi$, along the chord, $l_2(x)$ produces a uniform upwash $\alpha_{e2} = -C_{L2}/2\pi$, of the same amount so that the plate at zero incidence is, in fact, a streamline. Thus, for $\alpha = \alpha_{e1} + \alpha_{e2} = 0$, we have $C_{L1} = C_{L2}$. The first component distribution is given by the well-known relation due to Birnbaum:

$$l_1(x) = -\Delta C_p(x) = +\frac{2}{\pi}C_{L1}\left(\frac{1-x}{x}\right)^{1/2} \quad .. \quad .. \quad .. \quad .. \quad (1)$$

where ΔC_p is the difference between the pressure coefficients $C_p = (p - p_0)/(\frac{1}{2}\rho V_0^2)$ on the upper and lower surfaces of the aerofoil. The second component distribution is then:

$$l_2(x) = l_1(1-x) = \frac{2}{\pi}C_{L2}\left(\frac{x}{1-x}\right)^{1/2} \quad .. \quad .. \quad .. \quad .. \quad .. \quad (2)$$

The overall lift coefficient:

$$C_L = \int_0^1 l(x)\,dx = C_{L1} + C_{L2} = 2C_{L1} \quad .. \quad .. \quad .. \quad .. \quad .. \quad (3)$$

can be freely chosen.

The chordwise loading $l_1 + l_2$ is shaped like a ' saddleback ', as shown in Fig. 1. There is a suction force at the leading edge, to which only $l_1(x)$ contributes:

$$C_{T1} = -\frac{C_{L1}^2}{2\pi} = -\frac{C_L^2}{8\pi}\,; \quad .. \quad .. \quad .. \quad .. \quad .. \quad .. \quad (4)$$

and another suction force in the other direction at the trailing edge, to which only $l_2(x)$ contributes. This is equal and opposite to C_{T1} so that there is no overall drag.

In contrast to the aerofoil of infinite span, the wing of finite aspect ratio possesses streamwise vorticity components, both on the wing surface and in the wake, and these together induce a downwash over the wing surface. If the aspect ratio of the wing is large, this downwash is constant along the wing chord and if we assume further that the plan-form is such as to give the smallest induced drag, this downwash is constant along the span also, *i.e.*, it is constant over the whole wing surface. It is then possible to put the wing at the same incidence, namely:

$$\alpha = \alpha_i = \frac{v_z}{V_0} = \frac{1}{\pi A}\bar{C}_L \quad .. \quad .. \quad .. \quad .. \quad .. \quad .. \quad (5)$$

as is induced by the streamwise vortices. The same lift is then obtained as on the corresponding wing of infinite span at zero incidence, with the same saddleback chordwise loading and with

elliptic spanwise loading. This means that the suction forces at the leading and trailing edges still cancel one another; but there is now a drag component from the pressure forces normal to the surface, which is equal to:

$$\bar{C}_{Di} = \bar{C}_L \alpha = \bar{C}_L \alpha_i = \frac{1}{\pi A} \bar{C}_L^2 \quad .. \quad .. \quad .. \quad .. \quad .. \quad .. \quad (6)$$

by equation (5), as it should be for the wings considered, in the absence of a jet.

If the wing of finite aspect ratio is required to remain at zero incidence, the existence of a downwash contribution from the streamwise vorticity components means that the bound vortices $l_1(x)$, which on the two-dimensional aerofoil had to produce all the downwash needed, can now be weaker and are required to contribute only part of the downwash, as indicated in Fig. 2. The vortex distribution $l_2(x)$ is thus no longer equal to $l_1(1 - x)$. This implies that the chordwise loading becomes asymmetrical and that the suction forces at the leading and trailing edges do not cancel one another any more. In fact, C_{T1} is smaller than C_{T2} and it is in this manner that the induced drag occurs, in theory.

That the difference between leading-edge and trailing-edge suction has indeed the same value as the ordinary induced drag can be seen as follows. Consider an unswept wing of not too small an aspect ratio, so shaped as to give constant C_L values along the span and minimum induced drag. The overall tangential force is the sum of two components:

$$\bar{C}_T = C_{T1} + C_{T2} = -\frac{C_{L1}^2}{2\pi} + \frac{C_{L2}^2}{2\pi}$$

by equation (4), so that:

$$\bar{C}_T = \frac{1}{2\pi}(C_{L1} + C_{L2})(C_{L2} - C_{L1}) \, . \quad .. \quad .. \quad .. \quad .. \quad .. \quad (7)$$

On the other hand, the boundary condition on the wing reads $\alpha_{e1} + \alpha_{e2} + \alpha_i = 0$, where:

$$\alpha_{e1} = \frac{C_{L1}}{2\pi} \text{ and } \alpha_{e2} = -\frac{C_{L2}}{2\pi} \quad .. \quad .. \quad .. \quad .. \quad .. \quad .. \quad (8)$$

are the downwash angles belonging to the two bound vortex distributions and:

$$\alpha_i = \frac{\bar{C}_L}{\pi A} \quad .. \quad .. \quad .. \quad .. \quad .. \quad .. \quad .. \quad .. \quad (9)$$

with $\bar{C}_L = C_L = C_{L1} + C_{L2}$, is the downwash from the streamwise vortices. This leads to:

$$C_{L1} = \tfrac{1}{2}\bar{C}_L\left(1 - \frac{2}{A}\right) \text{ and } C_{L2} = \tfrac{1}{2}\bar{C}_L\left(1 + \frac{2}{A}\right) \quad .. \quad .. \quad .. \quad (10)$$

so that, by equation (7):

$$\bar{C}_T = \frac{1}{2\pi}\bar{C}_L \frac{2}{A}\bar{C}_L = \frac{1}{\pi A}\bar{C}_L^2 \quad .. \quad .. \quad .. \quad .. \quad .. \quad .. \quad (11)$$

as before. Accordingly,the same result is obtained for an aerofoil at any angle of incidence with any position of the stagnation points, which follows directly also from momentum and energy considerations.

The main advantage of producing a lift force with a saddleback chordwise distribution lies in the fact that, for an aerofoil of non-zero thickness, the velocity distribution is more uniform than it normally is with the aerofoil at an angle of incidence. For instance, the velocity peaks at the leading and trailing edges of the aerofoil are only about half as high as the single velocity peak at the leading edge of an aerofoil at incidence, at the same overall C_L value. The subsequent adverse pressure gradient behind the front peak can be slightly less steep for the aerofoil at zero incidence if it has about twice the lift. This implies that any breakdown of the flow associated with laminar-flow separation and subsequent bubble formation close to the leading edge, and

possibly loss of lift, should be delayed on the aerofoil at zero incidence (*i.e.*, with saddleback loading) until the lift is about twice that reached on the aerofoil at incidence. Thus the value of $C_{L\,\max}$ should be about twice as high for aerofoil shapes of moderate thickness-chord ratio (class B of Ref. 7). Further, the drag increment due to a breakdown of the flow at the leading edge, involving the loss of the suction force there, is also less since the suction force is only a quarter of that occurring at the wing at incidence with the same lift, by equation (4). However, there is also the possibility of a flow separation from the trailing edge, even if it is rounded and this is why such a flow never occurs in practice unless some external help is provided. Such a means is a jet which emerges from the lower surface near the trailing edge in that it makes it possible to maintain such a circulation at zero incidence. At the same time, the jet makes the solution unique and fixes the value of the circulation.

3. *Jet Effects on Thin Unswept Wings.*—Consider now the case of an aerofoil with a jet emerging from its lower surface somewhere near the trailing edge. The effects of such a jet on the circulation round the aerofoil and on the forces on it have been discussed in detail by D. A. Spence[2]. For the present purpose, we remind ourselves that the two principal effects of the jet are:

(*a*) It can establish an asymmetric flow and thus the natural circulation (as for the Thwaites flap), which would otherwise not be obtained because of viscosity effects

(*b*) It can increase the circulation beyond this value by virtue of its higher energy.

This is illustrated in Fig. 3. In the case of an aerofoil of elliptic section shape, say, any value of the circulation around the aerofoil at zero incidence is possible in an inviscid stream in the absence of the jet (Fig. 3a). In a viscous stream, a flow separation at the rear end is likely to prevent such a circulation altogether (Fig. 3b). A jet will at least help to establish the ' natural circulation ' which belongs to the rear stagnation point being at the jet exit. In fact, the jet may produce a ' supercirculation ' above the natural circulation (Fig. 3c), if the momentum of the jet is large and if flow separations are avoided. In the case of an aerofoil with a small flap, the natural circulation in inviscid flow (Fig. 3d) is likely to be reduced by viscosity effects (Fig. 3e), whereas a jet suitably discharged and making use of the Coanda effect may establish the natural circulation or even more (Fig. 3f).

In an analytical treatment of the inviscid flow past an aerofoil with jet, the jet may be replaced by a distribution of sources and vortices. These induce a velocity component normal to the aerofoil and, for the aerofoil to remain a stream surface, a vortex distribution along the aerofoil surface is required to cancel this upwash. The overall vorticity so added corresponds to the change in circulation and in lift force beyond the values which correspond to a position of the rear stagnation point at the jet exit. Now, it can be shown that the contribution of the sources to the upwash and hence to the pressure forces on the aerofoil is very small, except in the immediate neighbourhood of the jet exit. To a first approximation, the sources may, therefore, be ignored and the vortices only considered. Further, the jet may be assumed to be thin and the static pressure in the exit to be equal to the undisturbed pressure, p_0, so that the momentum of the air in the jet, M_J, remains constant along the jet. In that case, the aerofoil experiences a tangential force (parallel to the chord-line, *i.e.*, a thrust) along its external surfaces* (excluding the duct) of the magnitude:

$$C_T = \frac{T}{\frac{1}{2}\rho V_0^2 c} = -\,C_J(1 - \cos\tau)\,, \qquad \ldots\ \ldots\ \ldots\ \ldots\ \ldots \quad (12)$$

as shown by Maskell and Gates by means of the momentum theorem. Drag forces are called positive; τ is the discharge angle and:

$$C_J = \frac{M_J}{\frac{1}{2}\rho V_0^2 c} \qquad \ldots\ \ldots\ \ldots\ \ldots\ \ldots\ \ldots\ \ldots\ \ldots \quad (13)$$

* The forces considered throughout this note are always those acting along the external surfaces of the aerofoil, *i.e.*, they do not include the direct lift and thrust components of the jet, unless otherwise stated.

the jet momentum coefficient. The lift force, on the other hand, cannot be determined by the momentum theorem as it depends essentially on the penetration of the jet into the stream. It can be calculated numerically by the more detailed method of Spence who obtained for the lift force on the external surfaces of a thin aerofoil at zero incidence:

$$\frac{C_L}{\tau} = 2(\pi C_J)^{1/2} - C_J = 3{\cdot}54\sqrt{C_J} - C_J \quad .. \quad .. \quad .. \quad .. \quad (14a)$$

for small values of C_J and:

$$\frac{C_L}{\tau} = 3{\cdot}54C_J^{1/2} - 0{\cdot}675C_J + 0{\cdot}156C_J^{3/2} \quad .. \quad .. \quad .. \quad .. \quad (14b)$$

as an approximation for C_J values up to about 10. The chordwise distribution of this load and the vorticity distribution along the jet can also be determined in Spence's method.

In the following, we shall establish two simple approximate methods for calculating the chordwise distribution of the lift, as a supplement to Spence's more complicated method. The first is the simplest and only the overall lift can be made right whereas there is no external thrust force. In the second method, the thrust force given by equation (12) is also accurately represented.

The simplest approximation is obtained by assuming the lift distribution still to be symmetrical fore and aft, as in the case without jet. All the jet is supposed to do is to fix a certain circulation and thus a lift coefficient which can be taken from equation (14). In that case

$$l(x) = l_1(x) + l_2(x) \quad .. \quad .. \quad .. \quad .. \quad .. \quad .. \quad .. \quad (15)$$

as in equations (1) and (2), with $C_{L1} + C_{L2} = C_L$ and $C_{L1} = C_{L2}$, whereas $C_T = 0$. The shape of the stagnation streamlines and the chordwise lift distribution obtained in this way are shown in Fig. 4 (case b) and compared with the results from Spence's linearised theory (case a) for a typical example. It will be seen that even this crude approximation gives reasonable answers, considering that the behaviour of the solution from linearised theory in the region of the trailing edge is not quite correct either*.

To obtain a more refined solution, the chordwise loading must be asymmetric fore and aft so that the suction forces at the leading and trailing edges are no more equal and opposite but leave room for fulfilling the thrust condition (12). The simplest way of achieving the required asymmetry is to leave the two partial solutions l_1 and l_2 as they are and to add a third solution l_3. The latter must then be such that the downwash induced by it exactly compensates for the upwash induced by the jet vortices. It will suffice for the present purpose to assume that this upwash, α_{iJ}, is constant along the wing chord. The third partial solution is then:

$$l_3(x) = \frac{2}{\pi} C_{L3}\left(\frac{1-x}{x}\right)^{1/2} \quad .. \quad .. \quad .. \quad .. \quad .. \quad .. \quad (16)$$

It is of the flat-plate type, as $l_1(x)$. The downwash induced by it is constant along the chord and has the value $C_{L3}/2\pi$. Hence $\alpha_{e3} = C_{L3}/2\pi = -\alpha_{iJ}$. The total loading is then:

$$l(x) = l_1(x) + l_2(x) + l_3(x)\,, \quad .. \quad .. \quad .. \quad .. \quad .. \quad .. \quad (17)$$

with $l_1(x)$ from equation (1), $l_2(x)$ from equation (2) and $l_3(x)$ from equation (16).

---

* The correct behaviour of the velocity near the trailing edge is proportional to $(x = 1)^{n-1}$, with $\frac{1}{2} \leqslant n \leqslant 1$, depending on the discharge angle τ, *i.e.*, $n = \pi/(\tau + \pi)$, for the case of a jet emerging at the trailing edge. In contrast to this, the symmetrical loading (case *b*) always gives $n = \frac{1}{2}$; and the linearised theory gives a logarithmic infinity. The differences in the chordwise loading are similar to those found by Keune[6] for the case of a thin aerofoil with a hinged flap between the linearised solution of Glauert[7] and the exact solution.

It remains to determine the coefficients C_{L1}, C_{L2} and C_{L3}. This is possible without actually knowing how large α_{iJ} is. We use the streamline condition:

$$\alpha = \alpha_{e1} + \alpha_{e2} + \alpha_{e3} + \alpha_{iJ} = 0 , \quad .. \quad .. \quad .. \quad .. \quad .. \quad (18)$$

which leads to $\alpha_{e1} + \alpha_{e2} = 0$ since $\alpha_{e3} = -\alpha_{iJ}$. By equation (8), $\alpha_{e1} + \alpha_{e2} = (C_{L1}/2\pi) - (C_{L2}/2\pi) = 0$, and thus:

$$C_{L1} = C_{L2} , \quad .. \quad .. \quad .. \quad .. \quad .. \quad .. \quad .. \quad .. \quad (19)$$

i.e., $l_1 + l_2$ is still symmetrical fore and aft and represents a pure circulation. Further, for the overall lift:

$$C_L = C_{L1} + C_{L2} + C_{L3} , \quad .. \quad .. \quad .. \quad .. \quad .. \quad .. \quad (20)$$

where C_L may be taken from equation (14) or from experiment. Hence:

$$C_{L1} = C_{L2} = \tfrac{1}{2}(C_L - C_{L3}) \quad .. \quad .. \quad .. \quad .. \quad .. \quad .. \quad (21)$$

and it remains to determine C_{L3}. This can be done by considering the suction force at the leading edge:

$$-\frac{(C_{L1} + C_{L3})^2}{2\pi} = -\frac{1}{8\pi}(C_L + C_{L3})^2 , \quad .. \quad .. \quad .. \quad .. \quad .. \quad .. \quad (22)$$

which is not now equal and opposite to the suction force at the trailing edge:

$$\frac{C_{L2}^2}{2\pi} = \frac{1}{8\pi}(C_L - C_{L3})^2 . \quad .. \quad .. \quad .. \quad .. \quad .. \quad .. \quad .. \quad (23)$$

We may now consider the extreme case where the nozzle is so shaped that the thrust from equation (12) is all carried at the leading edge. Thus

$$C_T = -(1/8\pi)(C_L + C_{L3})^2 + (1/8\pi)(C_L - C_{L3})^2 = -C_J(1 - \cos\tau),$$

which gives a relation for C_{L3} if the overall lift and thrust coefficients are known:

$$C_{L3} = 2\pi\frac{C_J}{C_L}(1 - \cos\tau) . \quad .. \quad .. \quad .. \quad .. \quad .. \quad .. \quad (24)$$

C_{L1} and C_{L2} can then be calculated from equation (21) and hence the chordwise loading is known by equation (17). We have thus obtained a solution for the chordwise loading, including jet effects, without knowing the shape of the jet or the vorticity distribution along it. Stagnation streamlines and vortex distribution within the wing chord are in reasonable agreement with Spence's solution, as shown in Fig. 4, case (c).

Now, the jet-induced upwash, implied in this calculation, is by equation (24):

$$\alpha_{iJ} = -\alpha_{e3} = -\frac{C_{L3}}{2\pi} = -\frac{C_J}{C_L}(1 - \cos\tau) . \quad .. \quad .. \quad .. \quad .. \quad (25)$$

The jet may also induce a velocity component, v_{xJ}, parallel to the aerofoil chord. This will be the same on the upper and lower surfaces of the aerofoil and it does not, therefore, contribute to the lift force, to a first approximation. As the vorticity distribution along the jet is situated behind and below the aerofoil, we may assume v_{xJ} to be smaller than $\alpha_{iJ}V_0$. Taking it to be constant along the chord, we may put:

$$\frac{v_{xJ}}{V_0} = \varkappa\frac{C_J}{C_L}(1 - \cos\tau) , \quad .. \quad .. \quad .. \quad .. \quad .. \quad .. \quad (26)$$

with a factor $\varkappa$ of the order of 1 or smaller than that. As v_{xJ}/V_0 is a small term compared with unity, its value need not be known very accurately, and for estimation purposes we shall put $\varkappa = 0$ and, alternatively, $\varkappa = 1$ in later applications.

Proceeding to unswept wings of finite aspect ratio, we may consider the principal effect of the finite aspect ratio to be the existence of streamwise vorticity components both on the wing and in the jet. Thus, another additional downwash contribution, α_i, arises from the streamwise vortices. This is constant along the wing chord, as in the theory of Ref. 4, if the aspect ratio of the wing is large. We do not propose to go into any details here about how this downwash and the lift on the aerofoil can be determined but make use of results which will be published later by Maskell. Our aim is again to determine the chord and spanwise pressure distribution if the overall lift and thrust forces are known. For the present purpose it is sufficient to take the result of Maskell that the downwash has the value:

$$\alpha_i = \frac{\bar{C}_{L\,\mathrm{TOTAL}}}{\pi A + 2C_J} \qquad \ldots \ldots \ldots \ldots \ldots \ldots \ldots \quad (27)$$

for unswept wings of moderate and large aspect ratios with minimum induced drag, where $\bar{C}_{L\,\mathrm{TOTAL}}$ ($= \bar{C}_L$ for short) is the overall lift coefficient of the whole wing including the direct jet lift. If we consider again the extreme case that the whole external thrust occurs at the leading edge and not at the nozzle; and if we restrict ourselves to chordwise loadings of the type from equation (17), then it can be shown that the factor C_{L3} of the jet-induced loading contribution is still, to a first approximation, given by equation (24). Equation (21) for the coefficients C_{L1} and C_{L2}, however, must now be amended because α_i occurs as an additional term in equation (18). In the case of wings of high aspect ratio with weak jet where $C_J \ll \pi A/2$, so that:

$$\alpha_i = \frac{\bar{C}_L}{\pi A}, \qquad \ldots \ldots \ldots \ldots \ldots \ldots \ldots \quad (28)$$

equation (21) must be replaced by:

$$\left.\begin{aligned} C_{L1} &= \tfrac{1}{2}\bar{C}_L\left(1 - \frac{2}{A}\right) - \tfrac{1}{2}C_{L3} \\ C_{L2} &= \tfrac{1}{2}\bar{C}_L\left(1 + \frac{2}{A}\right) - \tfrac{1}{2}C_{L3} \end{aligned}\right\} \qquad \ldots \ldots \ldots \ldots \quad (29)$$

to take account of the finite aspect ratio. C_{L1}, C_{L2} and C_{L3} may be taken as being constant along the span for unswept wings of minimum induced drag.

This leads to an interesting answer for the special case of a wing with elliptic span loading and a 90-deg jet ($\tau = \pi/2$ and $\bar{C}_L = C_L$; $\bar{C}_J = C_J$). The crudest form of the thrust-drag balance, ignoring profile drag as well as any other additional drag, demands that the thrust, C_J, must be sufficient to overcome the induced drag which, in this case, may be approximated by:

$$\bar{C}_{Di} = \frac{\bar{C}_L{}^2}{\pi A}. \qquad \ldots \ldots \ldots \ldots \ldots \ldots \ldots \quad (30)$$

Hence $C_J = \bar{C}_L{}^2/\pi A$ and:

$$C_{L3} = \frac{2}{A}\bar{C}_L \qquad \ldots \ldots \ldots \ldots \ldots \ldots \ldots \quad (31)$$

by equation (24). We then find from equation (29) that $C_{L1} + C_{L3} = \frac{1}{2}\bar{C}_L$ and $C_{L2} = \frac{1}{2}\bar{C}_L$, so that the chordwise loading from equation (17) becomes:

$$l(x) = \frac{\bar{C}_L}{\pi}\left\{\left(\frac{1-x}{x}\right)^{1/2} + \left(\frac{x}{1-x}\right)^{1/2}\right\}, \qquad \ldots \ldots \ldots \quad (32)$$

i.e., the chordwise loading is again saddleback and symmetrical fore and aft, as in the case of an aerofoil at zero incidence without jet at the same overall $\bar{C}_L$. In other words: as expected, the jet puts just as much thrust back on to the leading edge as the suction there had been reduced to accommodate the induced drag (section 2). This result is of great practical importance for it implies that the principal advantage, the saddleback chordwise loading, can be maintained on wings of finite aspect ratio with jet.

In all other cases where $\tau < \pi/2$, or where part of the thrust is carried at the nozzle, the suction at the leading edge is less than that at the trailing edge, if the aerofoil is left at zero incidence to the main stream. To obtain the benefit of the saddleback loading, it is then necessary to put the aerofoil at a suitable positive angle of incidence. This should be one of the design conditions of an aircraft with jet flap.

The present approach has the advantage that it can easily be extended to wings of small aspect ratio and to swept wings, when the need arises (for swept wings, *see* section 7), because it can readily be incorporated into the theory of Ref. 4. Consider, for example, unswept wings of small aspect ratio. The induced incidence, α_i from equation (27), from the streamwise vortices increases by a downwash factor ω as the aspect ratio becomes smaller, with $\omega \to 1$ as $A \to \infty$ and $\omega \to 2$ as $A \to 0$. Whether α_{iJ} increases also has not yet been investigated. This is unlikely to occur since α_{iJ} is a sectional property. For wings of small aspect ratio the index $\frac{1}{2}$ in equations (1), (2) and (16) must be replaced by a parameter n, the value of which depends on the aspect ratio, with $\frac{1}{2} \leqslant n \leqslant 1$. Simultaneously, the effective incidence α_e as induced by the bound vortices is C_L/a rather than $C_L/2\pi$, where a is the sectional lift slope which depends on the aspect ratio of the wing; and the suction forces at the edges become C_L^2/a rather than $C_L^2/2\pi$. This would imply that the general conclusions are not affected by aspect-ratio effects although the numerical values of the various parameters are different from those for wings of large aspect ratio. For instance, the chordwise loading would remain saddleback but the suction peaks near the edges would become sharper since equation (32) is replaced by:

$$\bar{l}(x) = \frac{\sin \pi n}{2\pi n} \bar{C}_L \left\{ \left(\frac{1-x}{x} \right)^n + \left(\frac{x}{1-x} \right)^n \right\} \qquad \ldots \quad \ldots \quad \ldots \quad \ldots \quad (33)$$

and because n approaches unity as $A \to 0$. This would detract from the benefits of the creation of lift by means of a jet and, for this reason too, the jet-flap principle is more profitably applied to wings of moderate or large aspect ratio.

4. *Effects of Aerofoil Thickness.*—The relations derived so far apply to aerofoils of zero thickness, thin flat plates as a rule, where tangential forces appear as infinitely high suctions on infinitely small areas. In reality all such shapes must be rounded to avoid flow separations. The suction in then finite and distributed over a wider area, but the magnitude of the tangential forces is not primarily affected by a non-zero wing thickness. It is the lift force that is affected in the first place.

The present results can readily be extended to aerofoils of non-zero thickness if the method of Weber[8], 1953, is used. If $l(x)$ from equation (17) is considered to be the solution for the thin aerofoil, then the pressure distribution along the surface of the thick aerofoil is given by:—

$$C_p = 1 - \frac{1}{1 + \{S^{(2)}(x)\}^2} \left[\begin{array}{l} \cos \alpha' \{1 + S^{(1)}(x) + v_{xJ}/V_0\} \pm \\ \left\{ \left(\frac{C_{L1}}{2\pi} + \frac{C_{L3}}{2\pi} + \sin \alpha' \right) \sqrt{\left(\frac{1-x}{x} \right)} + \frac{C_{L2}}{2\pi} \sqrt{\left(\frac{x}{1-x} \right)} \right\} \{1 + S^{(3)}(x)\} \end{array} \right]^2 . \qquad (34)$$

$S^{(1)}(x)$, $S^{(2)}(x)$ and $S^{(3)}(x)$ are functions of the shape $z(x)$ of the aerofoil. This relation is derived from equation (3.30) of Ref. 8. The term $1 + S^{(1)}(x) + v_{xJ}/V_0$ follows from linearised theory for that part of the velocity increment which is the same on both surfaces, *i.e.*, it includes the pure thickness effect without lift as well as the velocity increment v_{xJ}/V_0 due to the jet (mainly mixing; *see* section 5 below). The term

$$\left(\frac{C_{L1}}{2\pi} + \frac{C_{L3}}{2\pi} + \sin \alpha' \right) \sqrt{\left(\frac{1-x}{x} \right)} + \frac{C_{L2}}{2\pi} \sqrt{\left(\frac{x}{1-x} \right)}$$

is the contribution of the vortex distribution along the chord for the thin aerofoil, as determined before. The factor $1 + S^{(3)}(x)$ represents a second-order correction to the lift term due to thickness, the full derivation of which has been given in Ref. 8. The denominator $1 + \{S^{(2)}(x)\}^2$ is again a second-order correction due to thickness, which matters mainly near the leading

and trailing edges and eliminates the infinite suction peaks which occur in thin-aerofoil theory. For elliptic sections, these corrections are exact. α' is the angle of incidence of the aerofoil in two-dimensional flow. α' may be interpreted as the effective incidence of a section on an unswept wing of finite span, provided the aspect ratio is not too small. α' is then given by the relation:

$$\alpha' = \frac{1}{2\pi}(\alpha - \alpha_i)a_J \,, \qquad \ldots \qquad (35)$$

where

$$a_J = \left(\frac{\partial C_L}{\partial \alpha}\right)_{\text{lin. th.}} \qquad \ldots \qquad (36)$$

is the value of the sectional lift slope as determined for the thin aerofoil from Spence's theory[2]. v_{xJ} is given by equation (26) or equation (44), and α_i by equation (27).

Equation (34) can be used in the following way for an unswept wing of moderate or large aspect ratio. We assume C_J, τ and $\bar{C}_L$ to be given. A calculation of the induced angle of incidence α_i then determines the spanwise loading* $C_L(y)$, the effective angle of incidence, $\alpha_e = \alpha - \alpha_i$, and also the geometric angle of incidence, α, which is needed to produce the required lift. From the values of $C_L(y)$ and α_e, it can be determined how much of this lift is due to the effective incidence and how much due to the jet effect at zero incidence by using Spence's result in the form:

$$C_L(y) = C_L(\alpha_e = 0) + C\alpha_e \,, \qquad \ldots \qquad (37)$$

with $C_L(\alpha_e = 0) = \sqrt{(3{\cdot}54C_J)}\tau$ as a rough approximation by equation (14) and $C = a_J$. $C_L(\alpha_e = 0)$ is then the value to be inserted for C_L into equations (21) and (24) and thus C_{L1}, C_{L2} and C_{L3} can be determined, the values of which are needed in evaluating equation (34). This procedure ensures that, although flat-plate distributions are used throughout as an approximation, the jet effects on the sectional lift and lift slope as well as on the induced downwash are properly represented. Alternatively, the value of α' in equation (34) may be so determined as to lead to the required lift force, whereas C_{L3} is determined so as to give the required thrust force (this is used in calculating the results in Fig. 9 below).

For aerofoils of elliptic section shape, an exact solution can be given:

$$C_p = 1 - \frac{1}{1 + \left(\frac{t}{c}\right)^2 \frac{(1-2x)^2}{1-(1-2x)^2}} \left[\cos\alpha' \left(1 + \frac{t}{c} + \frac{v_{xJ}}{V_0}\right) \pm \left\{ \left(\frac{C_{L1}}{2\pi} + \frac{C_{L3}}{2\pi} + \sin\alpha'\right) \sqrt{\left(\frac{1-x}{x}\right)} + \frac{C_{L2}}{2\pi} \sqrt{\left(\frac{x}{1-x}\right)} \right\} \left(1 + \frac{t}{c}\right) \right]^2 , \qquad (38)$$

where t/c is the thickness-chord ratio of the aerofoil. In equations (34) and (38) the different signs in the numerator refer to the two different surfaces of the aerofoil.

An important effect of the non-zero aerofoil thickness is that the sectional lift, as obtained by integration from:

$$C_L = -\int_0^1 (C_{p\,\text{US}} - C_{p\,\text{LS}})\, dx \qquad \ldots \qquad (39)$$

is not the same as $C_{L1} + C_{L2} + C_{L3} + a_J\alpha_e = C_{L\,\text{thin}}$ for the thin aerofoil. For elliptic section shapes:

$$C_L = \left(1 + \frac{t}{c}\right) C_{L\,\text{thin}} \,, \qquad \ldots \qquad (40)$$

---

* In such a calculation according to the method of Ref. 4, it is advisable to insert for the sectional lift slope, a, the value a_J from equation (36) and to multiply the downwash integral by the factor $1/(1 + 2C_J/\pi A)$ according to equation (27).

whereas the factor $1 + t/c$ becomes approximately equal to $1 + 0{\cdot}8t/c$ for sections with sharp trailing edge. This means that the lift can be appreciably higher on the thick aerofoil than on the thin aerofoil, in the absence of viscosity effects. This lift increase becomes even more important on swept wings where the factor $1 + t/c$ must be replaced by $1 + \{(t/c)/\cos\varphi\}$ which is the exact value for the sheared wing of infinite span with elliptic section. The relations are exact only when the chordwise loading of the thin aerofoil is of the type $l(x)$ from equation (17). They have been used as an approximation by Spence[2] for the different type of loading obtained from linearised theory, but in view of the small difference between this loading and $l(x)$, the resulting error should be small. This is borne out by the experiment where the lift increase due to thickness is evident.

5. *Some Examples and Comparison with Experiment.*—Before comparing calculated and measured pressure distributions, we may briefly consider possible effects of the viscosity of the stream. In the first place, the existence of a boundary layer along the aerofoil surfaces means that the jet is enveloped in a wake of reduced energy. Thus the asymmetry of the flow (up and down) may be affected and with it the circulation. We may expect this to influence mainly the integrated lift coefficient C_L for a given C_J but not so much the chordwise distribution of the load for a given C_L, so that calculated loadings should agree reasonably well with the measured ones if the overall C_L is taken from experiment. Flow separations, on the other hand, can have much more drastic effects. They may occur, on an aerofoil with a jet emerging from the lower surface near the trailing edge, immediately behind the leading edge and on either side of the nozzle, since in each of these places a large adverse pressure gradient is predicted by inviscid-flow theory. The effect of any such separation must be apparent as a deviation between calculated and measured pressure distributions. Thus the flow separation upstream of the nozzle, which is likely to occur for any values of C_J, τ and α, must show up in that the calculated stagnation pressure is never reached in practice. The flow separation at the trailing edge is likely to be the more pronounced as τ increases and to appear as a reduction of the calculated suction peak there. This implies that it is very difficult to check on the behaviour of the chordwise loading near the trailing edge by experimental means. A laminar separation near the leading edge is most likely to result in the formation of a separation bubble and thereby produce large but easily recognisable deviations between theoretical and measured pressure distributions. In practice, the existence of a bubble near the leading edge implies that the suction force there is largely lost and this is equivalent to a drag increment of the order:

$$C_D = \frac{C_L^2}{8\pi\cos\varphi} \qquad \ldots\ldots\ldots\ldots\ldots\ldots\ldots\ldots \quad (41)$$

on wings of moderate or large aspect ratios. This would appear to be inadmissible on wings with jet flap where one aspires to obtain high C_L values.

Lastly, possible effects of turbulent mixing may be mentioned. These may reduce the pressure in the immediate neighbourhood of the nozzle but the magnitude can be expected to be small (*see* Ref. 9, p. 100). Experimental results with a cold circular jet suggest the following relation for the pressure decrement or the velocity increment:

$$\frac{\Delta p}{\frac{1}{2}\rho V_0^2} = -\,0{\cdot}01\left(\frac{V_e}{V_0} - 1\right); \text{ or } \frac{v_x}{V_0} = +\,0{\cdot}005\left(\frac{V_e}{V_0} - 1\right), \qquad \ldots\ldots \quad (42)$$

where V_e is the mean velocity in the exit. In the simplified case where the momentum is assumed to be constant along the jet, C_J as defined by equation (13) is related to the exit velocity ratio V_e/V_0 by:

$$C_J = 2\frac{\delta}{c}\left(\frac{V_e}{V_0}\right)^2, \qquad \ldots\ldots\ldots\ldots\ldots\ldots\ldots \quad (43)$$

δ being the width of the jet at the exit. Hence equation (43) becomes:

$$\frac{\Delta p}{\frac{1}{2}\rho V_0^2} = -0{\cdot}01\left\{\sqrt{\left(\frac{C_J}{2\delta/c}\right)} - 1\right\} \text{ or } \frac{v_x}{V_0} = +0{\cdot}005\left\{\sqrt{\left(\frac{C_J}{2\delta/c}\right)} - 1\right\}. \qquad (44)$$

For a jet issuing from somewhere close to the trailing edge, such a velocity increment may be expected to appear on both surfaces of the aerofoil, falling off slowly as the distance from the trailing edge increases. Turbulent mixing may also be considered as a means of augmenting the thrust but the range of useful application of such thrust augmentors appears to be restricted to assistance at take-off (*see* Ref. 9).

The method for calculating the pressure distribution has been applied to two cases where experimental results are available from tests by Dimmock[10]. The aerofoil section was an ellipse with $t/c = 0{\cdot}125$ and the exit was located on the lower surface about 1 per cent of the wing chord upstream of the trailing edge, the nozzle width being about $0{\cdot}002c$ and the discharge angles nominally 30 deg and 90 deg ($31{\cdot}4$ deg and $90{\cdot}0$ deg exactly). The model was so mounted that the flow was very nearly two-dimensional. The results are reproduced in Figs. 5 and 6. Fig. 8 contains results from a French test on a NACA 0018 section which was shortened to 90 per cent of its original chord, with a jet issuing at 58 deg again from the lower surface near the trailing edge. All these tests were made at low speeds ($M_0 \ll 1$).

Equation (34) has been used for the calculation, equation (38) for the special case of the elliptic section. In general, the results confirm the theoretical approach in that the shape is nearly saddlebacked, there being no great difference between the two different methods of the present paper nor between these and Spence's solution[2]. The usefulness of this shape of the chordwise loading, in comparison with creating the same lift by means of an angle of incidence and no jet, is clearly demonstrated in Fig. 6d. The effect of the thickness of the aerofoil is quite considerable as can be seen from Fig. 6c where the results from the full calculation are compared with what is obtained from thin-aerofoil theory. The infinite suction peaks of the thin aerofoil especially make any design work impossible and for this purpose the inclusion of thickness effects is vital.

The full lines in Figs. 5, 6 and 8 have been calculated on the assumption that the thrust C_T from equation (12) is carried at the leading edge, with C_{L3} from equation (24). Dashed lines are shown in Figs. 6d and 6e, which have been calculated on the assumption that the external thrust acts at the exit and not at the leading edge, i.e., $C_{L3} = 0$. Fig. 8 has also been computed under this assumption, and the asymmetry (fore and aft) of the pressure distribution in this case is entirely due to the thickness distribution $z(x)$ which thus proves to be an important parameter. In general it will be seen that the experimental results lie about half-way between the two estimates (with and without C_{L3}) and do not, therefore, give a conclusive indication of which is to be preferred.

The value of C_J in equation (24) has been taken as the overall thrust measured on the balance. This is considerably less than the value of the momentum coefficient quoted in the figures of Ref. 10, especially in the case $\tau = 90$ deg. This thrust loss is obviously a consequence of flow separations. Taking the full theoretical value of the thrust when determining C_{L3} from equation (24) must give the wrong answer for the pressure distribution, as it is seen to do in Fig. 5f.

The comparison between measured and calculated pressures gives some very clear indications of the effects of flow separations. A typical case of a laminar separation from the leading edge, with the formation of a long bubble, is shown in Fig. 6f. There is evidently little loss of lift but a loss in the thrust component of the normal pressure force. On the other hand, the suction inside the bubble ($C_p \simeq -3{\cdot}5$ in this case) is uncommonly high for a bubble of this length as compared with what is normally found for aerofoils, at incidence (*see*, for example, McCullough and Gault[11], 1951). This means that there is still some tangential force left and that the drag estimate according to equation (41) may well be pessimistic. This effect may be explained from the physical picture of the flow as suggested by Norbury and Crabtree[12]. According to this, the pressure coefficient C_{p1}, in the constant pressure part of the bubble is such that the pressure recovery through turbulent mixing is just large enough to bring the static pressure back to the

ambient pressure, p_0, or to some other value, C_{p2}, if the flow re-attaches to the surface. It is also suggested that the pressure recovery coefficient:

$$\sigma = \frac{p_2 - p_1}{\frac{1}{2}\rho V_1^2} = \frac{C_{p2} - C_{p1}}{1 - C_{p1}}$$

is of the order of $0{\cdot}4$. This is confirmed by the example of Fig. 6f where $C_{p1} = -3{\cdot}5$ and $C_{p2} = -1{\cdot}7$ (the station 2 being where the actual pressure distribution joins the one calculated for attached flow, which is fairly well defined here). Hence $\sigma = 0{\cdot}40$. The high suction in the bubble is therefore to be explained by the relatively high value of C_{p2} which in turn is a consequence of the saddleback loading for attached flow. Thus this special type of loading has a beneficial effect even after the flow has separated from the nose in that it makes high suctions and thereby shorter bubbles possible, compared with bubbles observed on aerofoils at incidence without a jet where the bubble growth is much more rapid.

Another beneficial effect of the saddleback loading, with its implied suction peak near the trailing edge, is that greater thickness/chord ratios may be used than is possible on an aerofoil at incidence. The latter suffers from its tendency towards rear separations and there is thus a limit to the use of round-nosed or drooped-nose shapes because, even if the leading-edge separation is thereby avoided, a rear separation will occur. In the case of the aerofoil with jet, the adding of thickness, or camber, near the leading edge can be carried further because the rear separation is postponed by the jet.

It is of interest to note in this context that evidence of a flow separation from the upper surface near the trailing edge is consistently apparent for the case with 90-deg jet in Fig. 5. This reduces the trailing-edge suction but does not eliminate it, so that it still appears possible to use leading-edge thickness and camber to delay the onset of the leading-edge separation further than on an aerofoil at incidence (*i.e.*, to more than twice the C_L value); and to benefit from a slower growth of the bubble, once separation has occurred.

The effect of a flow separation on the lower surface upstream of the nozzle shows up in all cases in that the main-stream stagnation pressure is never reached. However, there appears to be a noticeable effect of the presence of the jet and of its direction. Whereas, on ordinary aerofoils without jet, the pressure coefficient at the trailing edge normally reaches a value of about $C_p = +0{\cdot}1$ (it should have been $+1{\cdot}0$ again, in inviscid flow, for finite trailing-edge angles), we find for the 30-deg jet values of about $+0{\cdot}2$ and sometimes more; and for the 90-deg jet still higher values up to about $+0{\cdot}6$. This remains to be investigated. However, neither method can describe the conditions near the jet exit with any accuracy. For that, a different approach is needed altogether.

The experimental results indicate quite clearly that the mean values of the velocities on the upper and lower surfaces, at the mid-chord point, say, are not the same for the various jet thrust values. Without jet, this mean value depends only on the thickness distribution of the aerofoil section, to a first approximation, if the aerofoil is in a uniform stream of velocity V_0. With a jet, a tangential velocity increment, v_{xJ}, may be induced, as explained above, and this has been taken into account in equations (34) and (38) and in the examples in Figs. 5 and 6. Here, v_{xJ} has been replaced by a mean value over the chord and this has been taken from equation (44). Fig. 7 confirms again that v_{xJ} does exist and that the estimates from equations (26) and (44) are of the right order, if $\varkappa = 1$ in equation (26). However, only the empirical estimate based on a mixing process, from equation (44), has a sound physical interpretation whereas the other has not, since $\varkappa = 1$ seems far too extreme. Thus the agreement with equation (26) may be considered as fortuitous. The experiments, therefore, seem to indicate the existence of a small but significant mixing process and this merits further investigation.

It would seem that the reduction of the pressures due to mixing is also responsible for the discrepancies between measured values in Fig. 6d and values calculated by means of an electrolytic tank by Malavard*. The latter are consistently below the measured pressures over most of the chord and the discrepancy is of the same order as the reduction due to mixing shown in Fig. 7.

* These results have not yet been published and have kindly been put at our disposal.

Finally, a comparison has been made in Fig. 9 between a theoretical pressure distribution and one measured on a wing of finite aspect ratio by Williams and Alexander[16]. In this case, equation (34) has been used and lift and thrust forces have been made the same as in the experiment. Thus the effect of the finite span has been taken into account only by adjusting the component distribution $l_1(x)$, as explained in section 2, *i.e.*, the effective angle of incidence has been reduced. Fig. 9 shows that this procedure accounts for most of the observed effects. The suction peak near the leading edge is considerably reduced whereas that near the trailing edge remains largely unaltered. There is, however, a systematic discrepancy near the leading edge, the measured loading being peakier than that calculated from two-dimensional flat-plate distributions. This may well be a genuine effect of the relatively small aspect ratio of the model tested ($A = 2{\cdot}75$). A peakier loading with the load concentrated nearer to the edges is to be expected from the argument which led to equation (33). It is comforting to know, however, that this effect is still relatively insignificant even at so low an aspect ratio.

6. *Effects of Camber.*—In any practical application of the aerofoil with jet, it is desirable to avoid a separation of the laminar boundary layer from somewhere near the leading edge throughout the working range, in spite of possible benefits due to the jet, which may be present even after the flow has separated. With the pressure distribution known for attached flow near the leading edge, the separation point can be estimated and, with the aid of Owen's criterion (*see* Ref. 13), we can also decide whether a long bubble, like that in Fig. 6f, is likely to occur. As a much cruder rule, we can take the suction peak itself as an indication of whether separation is likely to occur or not, and we may assume that the minimum pressure coefficient will not go appreciably below a value of about -10 for symmetrical aerofoil sections. In Dimmock's tests[10] the highest measured values (which do not necessarily represent the minimum pressure however), were about $C_p = -6{\cdot}5$. It appears worthwhile, therefore, to consider the effect of modifications to the leading edge, which will delay the formation of a long bubble, as there is no reason why an aerofoil with jet should be symmetrical. Among the various possibilities, such as leading-edge thickness and droop, kinked nose, nose flap, air injection, we consider here the simplest case of applying camber to the whole areofoil.

Camber is used to reduce the sharp suction peak near the nose, for a given C_L, and the family of camber-lines, which has been derived by Brebner[14] appears to be most suited for the present purpose. Because of the high slope of these camber-lines near the nose, they are most effective in reducing suction speaks there. Brebner's family of camber-lines leads to functions $\gamma(x)$ of the chordwise vorticity distribution, which are tabulated in Ref. 14. With these, the pressure distribution along the surface of an aerofoil of non-zero thickness can be obtained from:

$$C_p = 1 - \frac{1}{1 + \{S^{(2)}(x)\}^2}\left[\begin{array}{l}\cos\alpha'\left\{1 + S^{(1)}(x) + \dfrac{v_{xJ}}{V_0} \pm \dfrac{\gamma(x)}{2V_0}\right\} \pm \\ \left\{\left(\dfrac{C_{L1}}{2\pi} + \dfrac{C_{L3}}{2\pi} + \sin\alpha'\right)\sqrt{\left(\dfrac{1-x}{x}\right)} + \dfrac{C_{L2}}{2\pi}\sqrt{\left(\dfrac{x}{1-x}\right)}\right\}\left\{1 + S^{(3)}(x)\right\}\end{array}\right]^2, \tag{45}$$

which contains equation (34) as the special case of symmetrical sections, $\gamma - 0$. The overall lift coefficient must now be obtained by integration,

$$C_L \simeq C_N = -\int_0^1 \Delta C_p \, dx$$

from the difference between the pressure coefficients on the two surfaces:

$$-\Delta C_p = l(x) = 4\,\frac{\cos\alpha'\left\{1 + S^{(1)}(x) + \dfrac{v_{xJ}}{V_0}\right\}}{1 + \{S^{(2)}(x)\}^2} \times$$

$$\times\left[\cos\alpha'\frac{\gamma(x)}{2V_0} + \left\{\left(\frac{C_{L1}}{2\pi} + \frac{C_{L3}}{2\pi} + \sin\alpha'\right)\sqrt{\left(\frac{1-x}{x}\right)} + \frac{C_{L2}}{2\pi}\sqrt{\left(\frac{x}{1-x}\right)}\right\}\left\{1 + S^{(3)}(x)\right\}\right]. \tag{46}$$

An explicit relation for the lift can be given for the special case of an aerofoil of elliptic section shape with v_{xJ} = constant and $\gamma(x)/2V_0 = 4{\cdot}53f/c$ = constant, where f is the maximum camber of the section. This is a cambered aerofoil with the same ' constant-load ' camber-line as the one denoted by N.A.C.A. as $a = 1$. The application of such a camber-line may be more reasonable in the case with jet than for ordinary aerofoils. In the latter case, local flow separations just upstream of the trailing edge detract considerably from the benefit obtained by camber, whereas this need not occur as severely on the aerofoil with jet. Moreover, the fore and aft symmetry of this camber-line goes well with the saddleback loading. For the ' constant-load ' camber-line:

$$C_N = 18{\cdot}1\cos^2\alpha'\left(1+\frac{t}{c}+\frac{v_{xJ}}{V_0}\right)\left[\frac{1}{1-t/c}-\frac{(t/c)^2}{2\sqrt{\{1-(t/c)^2\}^3}}\ln\frac{1+\sqrt{\{1-(t/c)^2\}}}{1-\sqrt{\{1-(t/c)^2\}}}\right]\frac{f}{c}+$$

$$+\cos\alpha'\left(1+\frac{t}{c}+\frac{v_{xJ}}{V_0}\right)(C_{L1}+C_{L2}+C_{L3}+2\pi\sin\alpha') \quad .. \quad .. \quad .. \quad .. \quad (47)$$

Note that both thickness/chord ratio and camber now enter the relation in a complicated manner. However, camber leads to a lift increment only and does not affect the lift slope C_L/α, to a first order, as for ordinary aerofoils. The jet does affect the lift slope in the same way as for the thin aerofoil, equation (40) and through the small term v_{xJ} such that, to a first approximation:

$$\frac{C_L - C_{L0}}{\alpha} = \left(1+\frac{t}{c}+\frac{v_{xJ}}{V_0}\right)a_J \quad .. \quad .. \quad .. \quad .. \quad .. \quad .. \quad (48)$$

in this particular case, C_{L0} being the lift at zero incidence from equation (47).

That reasonable aerofoil shapes can be obtained in this manner is demonstrated in Fig. 10. This shows also how the occurrence of long bubbles can be delayed to higher values of the sectional lift coefficient by the use of camber. For example, C_L could be increased from about $2{\cdot}4$ to about $3{\cdot}2$ by 4 per cent camber if the limiting C_p value were -10, for the $12{\cdot}5$ per cent thick elliptic section considered. For thicker sections, the C_L values obtainable can be much higher.

7. *Possible Effects of Sweep.*—It would appear that swept wings open up another field where the jet-flap scheme may be employed with advantage. In general, swept wings suffer from the fact that the pressure distribution due to thickness and the chordwise loadings vary along the span, as explained in Ref. 4. For instance, the lift slope at the centre section of a sweptback wing is, in general, less and its chordwise distribution less peaky than at a station near mid–semi-span where the ' sheared-wing ' conditions are similar to those on a two-dimensional unswept aerofoil but for a factor of about $\cos\varphi$ to the sectional lift slope. Conversely, the lift slope is higher and its chordwise distribution peakier near the tips of a sweptback wing. This non-uniformity, due to essentially three-dimensional–flow phenomena, is at the root of many of the undesirable features of sweptback wings, such as premature flow separations and drag rises, as well as unstable pitching-moment characteristics.

With the addition of a jet, two further parameters are introduced which can be varied at will in an attempt to cure some of the unfavourable properties of the swept wing at their origins: the jet angle and the jet momentum. Both could suitably be varied along the span, depending on the angle of sweep. For example, stronger blowing at a higher angle in the centre region than near the tips could be used to make the loading more uniform. This might improve both the high-speed characteristics, by straightening the isobars, and the stalling characteristics, by reducing the suction peaks for a given lift and thus delaying premature flow separations in undesirable places. This might possibly be achieved up to C_L values which can, in principle, be twice as high as on the wing without jet. It would appear that such benefits cannot easily be achieved by any other known means.

Whether this can in fact be achieved in practice cannot yet be decided and requires further study. However, some peculiarities and difficulties can be pointed out already now, indicating the main problems to be tackled. These concern, as may be expected, again the centre and tip

regions. They can be demonstrated by considering the simple case of a swept wing of infinite span with circulation at zero incidence but without jet (the case that leads to the saddleback loading $l_1 + l_2$ for unswept wings, equations (1) and (2), as discussed in section 2).

On a swept wing, the downwash induced by the bound vortices at the centre-section can be approximated by:

$$\frac{v_z(x)}{V_0} = \frac{1}{4\pi}\left\{\int_0^1 l(x')\,\frac{dx'}{x - x'} + \pi \tan\varphi\, l(x)\right\}, \quad .. \quad .. \quad .. \quad .. \quad (49)$$

as has been shown in Ref. 4. This differs from the relation for the two-dimensional aerofoil by the second term. In the present case, the boundary condition reads $v_z = 0$, and an explicit solution with $l \to \infty$ at both edges can be found:

$$l(x) = l_1(x) + l_2(x) = \frac{1}{\pi} C_L \cos\varphi \left\{\left(\frac{1-x}{x}\right)^{n_0} + \left(\frac{1}{1-x}\right)^{1-n_0}\right\}, \quad .. \quad .. \quad (50)$$

where

$$n_0 = \tfrac{1}{2}\left(1 - \frac{\varphi}{\pi/2}\right) \quad .. \quad .. \quad .. \quad .. \quad .. \quad .. \quad .. \quad (51)$$

and hence

$$1 - n_0 = \tfrac{1}{2}\left(1 + \frac{\varphi}{\pi/2}\right).$$

The loading from equation (50) may be interpreted as the superposition of the loading of a swept-back wing (first term, l_1) and that of a swept-forward wing with x replaced by $1 - x$ (second term, l_2). This has far-reaching consequences.

In the first place, the lift coefficients of the individual distributions are no longer equal:

$$C_{L1} = \tfrac{1}{2}\left(1 - \frac{\varphi}{\pi/2}\right) C_L, \quad .. \quad .. \quad .. \quad .. \quad .. \quad .. \quad (52)$$

whereas

$$C_{L2} = \tfrac{1}{2}\left(1 + \frac{\varphi}{\pi/2}\right) C_L. \quad .. \quad .. \quad .. \quad .. \quad .. \quad .. \quad (53)$$

This implies that the loading is no longer symmetrical fore and aft. The aerodynamic centre is no longer at the mid-chord point:

$$\frac{x_{a.c.}}{c} = \tfrac{1}{2}\left(1 + \frac{\varphi}{\pi/2}\right), \quad .. \quad .. \quad .. \quad .. \quad .. \quad .. \quad .. \quad (54)$$

i.e., $x_{a.c.}/c = \frac{1}{2}$ only when $\varphi = 0$. For swept-back wings, it is further aft. For $\varphi = +45$ deg, we have $x_{a.c.}/c = \frac{3}{4}$.

For a thick aerofoil at zero incidence, the pressure distribution at the centre section is given by:

$$C_p = 1 - \frac{1}{1 + \{S^{(2)}(x)\}^2}\left\{1 + \cos\varphi S^{(1)}(x) - f(\varphi)\cos\varphi \frac{S^{(2)}(x)}{\sqrt{[1 + \{S^{(2)}(x)\}^2]}} \pm \tfrac{1}{2} l(x)\right\}^2, \quad .. \quad (55)$$

where $f(\varphi)$ is a function of the angle of sweep, which is tabulated in Ref. 15. $S^{(1)}(x)$ and $S^{(2)}(x)$ depend on the profile shape only. For elliptic sections, $S^{(1)}(x) = t/c = \text{const.}$; $S^{(2)}(x) = (t/c)[(1 - 2x)/\sqrt{\{1 - (1 - 2x)^2\}}]$, as in equation (38). Fig. 11 shows a few examples of pressure distributions. The asymmetry fore and aft and the sharp suction peaks near the trailing edge, which result from the second, swept-forward, distribution, can clearly be seen.

For a swept wing with jet, another load distribution will be needed, which corresponds to $l_3(x)$ of equation (16). This is to compensate for the upwash induced by the circulation of the jet. It cannot be of the form of l_1 from equation (50), since such a distribution (corresponding to an ordinary swept-back wing) does not produce a suction force at the leading edge, as has been shown in Ref. 6. In fact, $l(x)$ from equation (50) leads to a suction force at the trailing edge only and thus to an overall drag. This is the same behaviour as is known from ordinary swept-back wings. $l_3(x)$ must, therefore, be of the type $l_2(x)$ and it can be determined from the condition that the reduction of the suction force at the trailing edge is equal to the external jet thrust.

This procedure does not contradict that applied to unswept wings in section 3. The symmetry properties of the unswept aerofoil lead to the same result whether l_1 is increased or l_2 decreased, for the same sectional lift.

A calculation of $l_3(x)$ cannot yet be carried out since the suction forces of the individual distributions are not known. Theoretically, from equation (55) $C_{T1} = 0$ and $C_{T2} = \infty$. Whereas the theoretical result $C_T = 0$ for the swept-back wing is supported by experimental evidence, little is as yet known about swept-forward wings. There are indications that the suction force is twice as high as that of the corresponding sheared wing.

This leaves us with a number of problems which remain to be investigated. But we can at least conclude that the sectional properties of an aerofoil with jet cannot be carried over to the centre and tip regions of swept wings.

8. *Conclusions.*—The present treatment of the aerofoil with a jet emerging from its lower surface near the trailing edge is based on unpublished work by Gates, Maskell and Spence[2] and extends it by providing a simple method for calculating the pressure distribution over wings of non-zero thickness and finite aspect ratio. The main conclusions which can be drawn at the present stage are as follows:

(*a*) It is possible to estimate with reasonable accuracy the pressure distribution over the surface of any given thick aerofoil section with jet, except in the region of the nozzle, if the external lift coefficient C_L and the jet momentum coefficient are given. The method can readily be extended to wings of finite span and it provides a basis for a rational wing design, including cambered wings.

(*b*) Several aerodynamic advantages of the jet-flap system become apparent. The saddleback chordwise loading, which is typical of the aerofoil with jet, allows C_L values to be obtained without flow separation, which can be about twice as high as when the lift is created by means of putting the aerofoil at an angle of incidence. Further, this particular type of loading, with its rear suction peak not easily affected by flow separations, allows the use of thickness and camber near the leading edge to an extent which is not normally possible on ordinary aerofoils, whereby the lift obtainable is increased further. Lastly, when separation near the leading edge occurs, the resulting bubble can be shorter and the leading-edge suction higher than on ordinary aerofoils, again due to the basic saddleback loading.

(*c*) The scheme may be particularly suited for swept wings where a grading of the jet momentum and angle along the span can be used to reduce the disadvantages inherent in such wings. However, further work is required since the sectional properties of an aerofoil with jet cannot be carried over to the centre and tip regions of swept wings.

REFERENCES

No.	*Author*	*Title, etc.*
1	I. M. Davidson	The jet flap. *J. R. Aer. Soc.*, Vol. 60, p. 24. January, 1956.
2	D. A. Spence	The lift coefficient of a thin, jet-flapped wing. *Proc. Roy. Soc.* (*A*) Vol. 238, pp. 46-68. 1956.
3	B. Thwaites	The production of lift independently of incidence. The Thwaites flap. Parts I & II. R. & M. 2611. November, 1947.
4	D. Küchemann	A simple method for calculating the span and chordwise loading on straight and swept wings of any given aspect ratio at subsonic speeds. R. & M. 2935. August, 1952.
5	D. Küchemann	Types of flow on swept wings with special reference to free boundaries and vortex sheets. *J. R. Aer. Soc.*, Vol. 57, p. 683. November, 1953.
6	F. Keune	Auftriebs einer geknickten ebenen Platte. *L.F.F.*, Vol. 13, p. 85. 1936. Momente und Ruderauftriebs einer geknickten ebenen Platte. *L.F.F.*, Vol. 14, p. 558. 1937.
7	H. Glauert	Theoretical relationship for an aerofoil with hinged flap. R. & M. 1095. 1927.
8	J. Weber	The calculation of the pressure distribution over the surface of two-dimensional and swept wings with symmetrical aerofoil sections. R. & M. 2918. July, 1953.
9	D. Küchemann and J. Weber ..	*Aerodynamics of Propulsion.* McGraw-Hill Book Company, Inc. 1953.
10	N. A. Dimmock	An experimental introduction to the jet flap. Report N.G.T.E. R.175, A.R.C. 18,186. April, 1955.
11	G. B. McCullough and D. E. Gault.	Examples of three representative types of airfoil section stall at low speed. N.A.C.A. Tech. Note 2502. September, 1951.
12	J. F. Norbury and L. F. Crabtree	A simplified model of the incompressible flow past two-dimensional aerofoils with a long bubble type of flow separation. R.A.E. Tech. Note Aero 2352, A.R.C. 17,945. June, 1955.
13	L. F. Crabtree	The formation of regions of separated flow on wing surfaces. R.A.E. Report Aero 2528, A.R.C. 17,524. November, 1954.
14	G. G. Brebner	The application of camber and twist to swept wings in incompressible flow. C.P. 171. March, 1952.
15	D. Küchemann and J. Weber ..	The subsonic flow past swept wings at zero lift without and with body. R. & M. 2908. March, 1953.
16	J. Williams and A. J. Alexander	Three-dimensional wind-tunnel tests of a 30 deg jet flap model. C.P. 304. November, 1955.

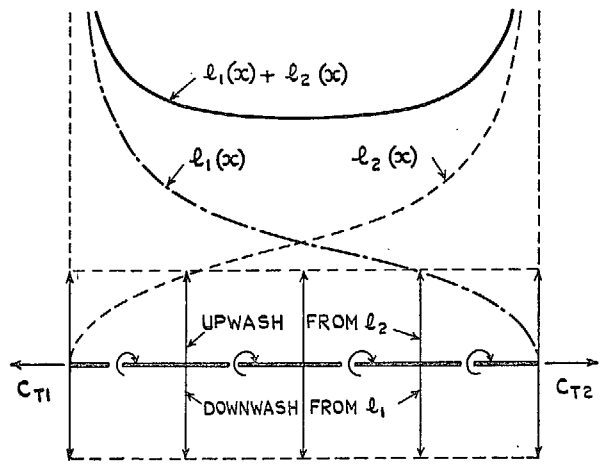

FIG. 1. Distribution of bound vorticity vector and of downwash for two-dimensional aerofoil at zero incidence with lift.

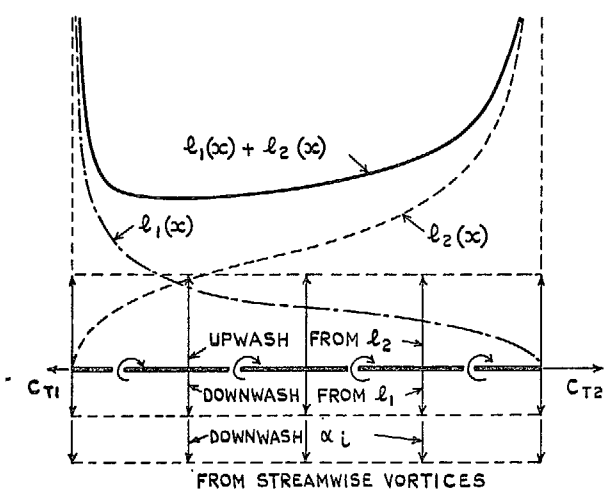

FIG. 2. Distribution of bound vorticity vector and of downwash for wing of finite span.

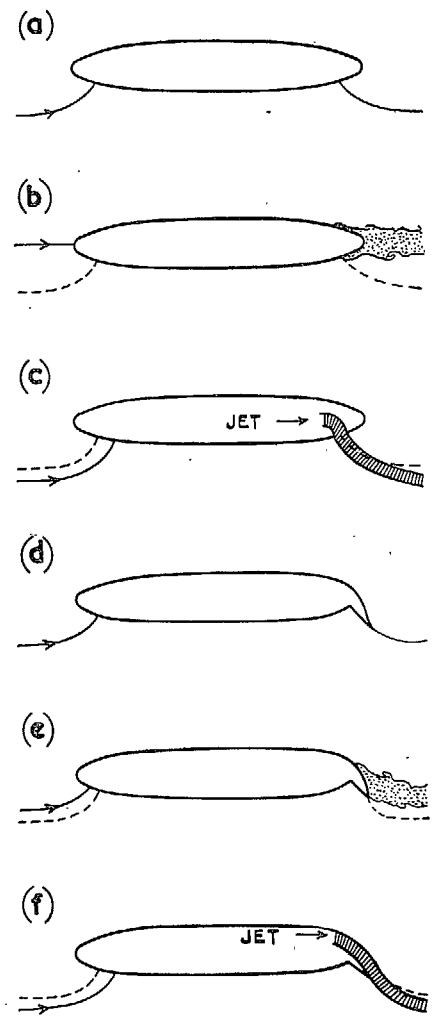

FIGS. 3a to 3f. Possible types of flow for aerofoils without and with jet.

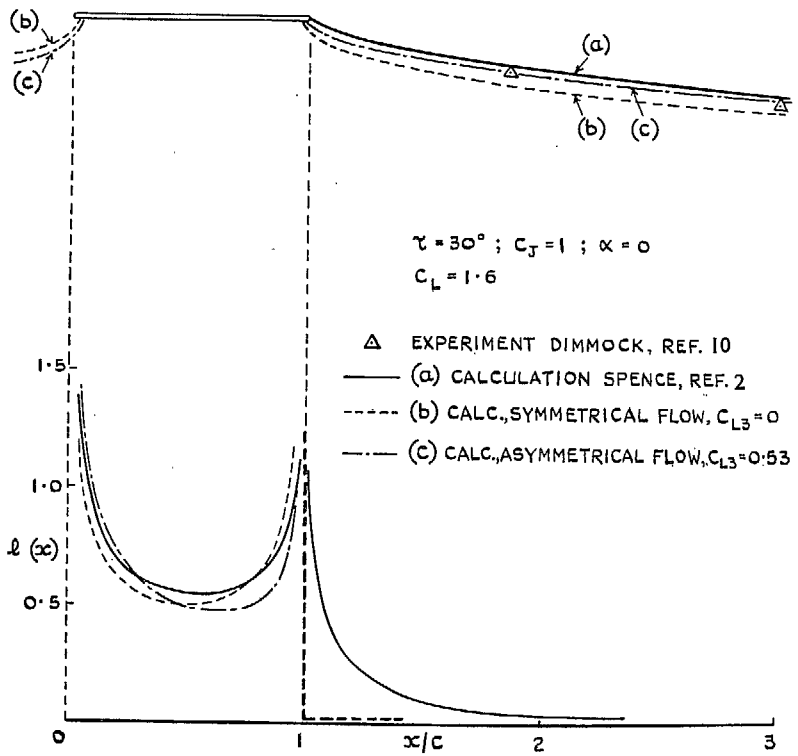

FIG. 4. Stagnation streamlines and chordwise vorticity distributions from various approximate theories.

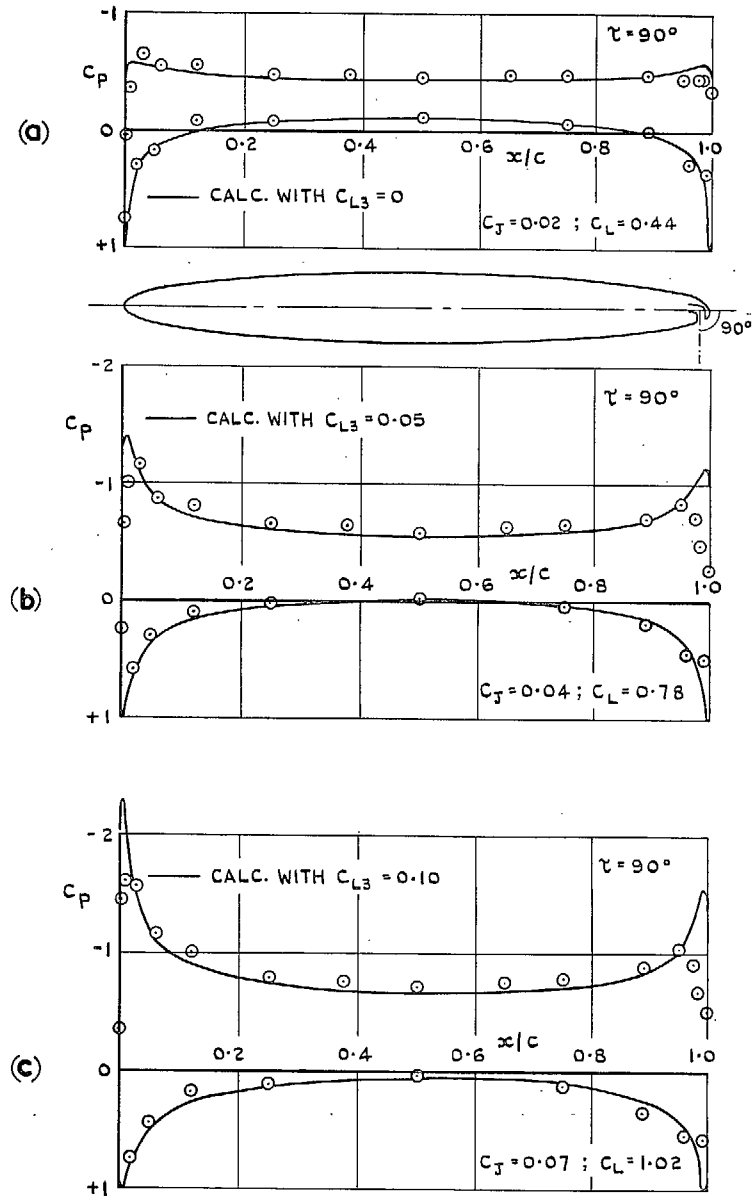

FIGS. 5a to 5c. Pressure distributions over an aerofoil with 90-deg jet (From Dimmock's tests[10]).

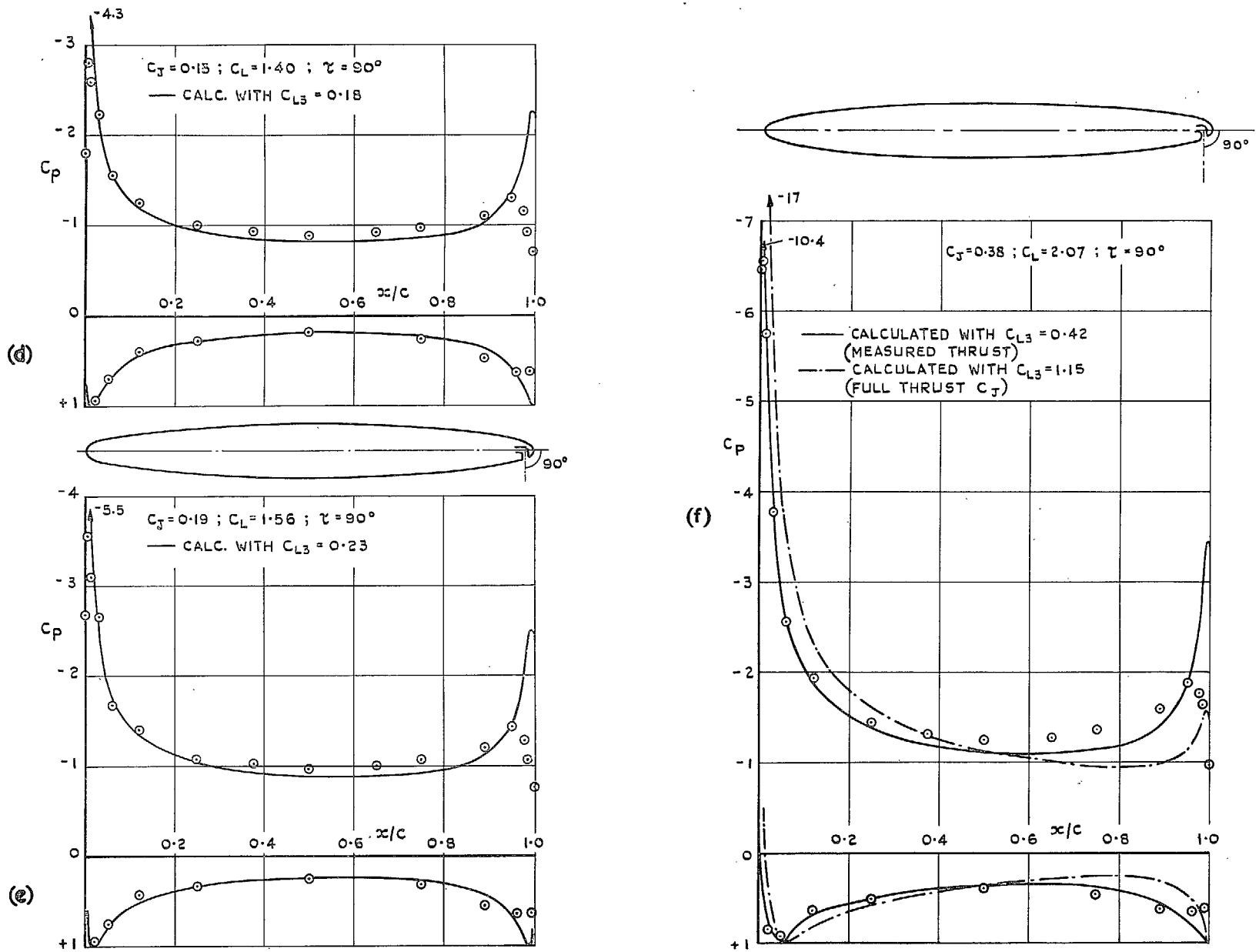

FIGS. 5d to 5f. Pressure distributions over an aerofoil with 90-deg jet (From Dimmock's tests[10]).

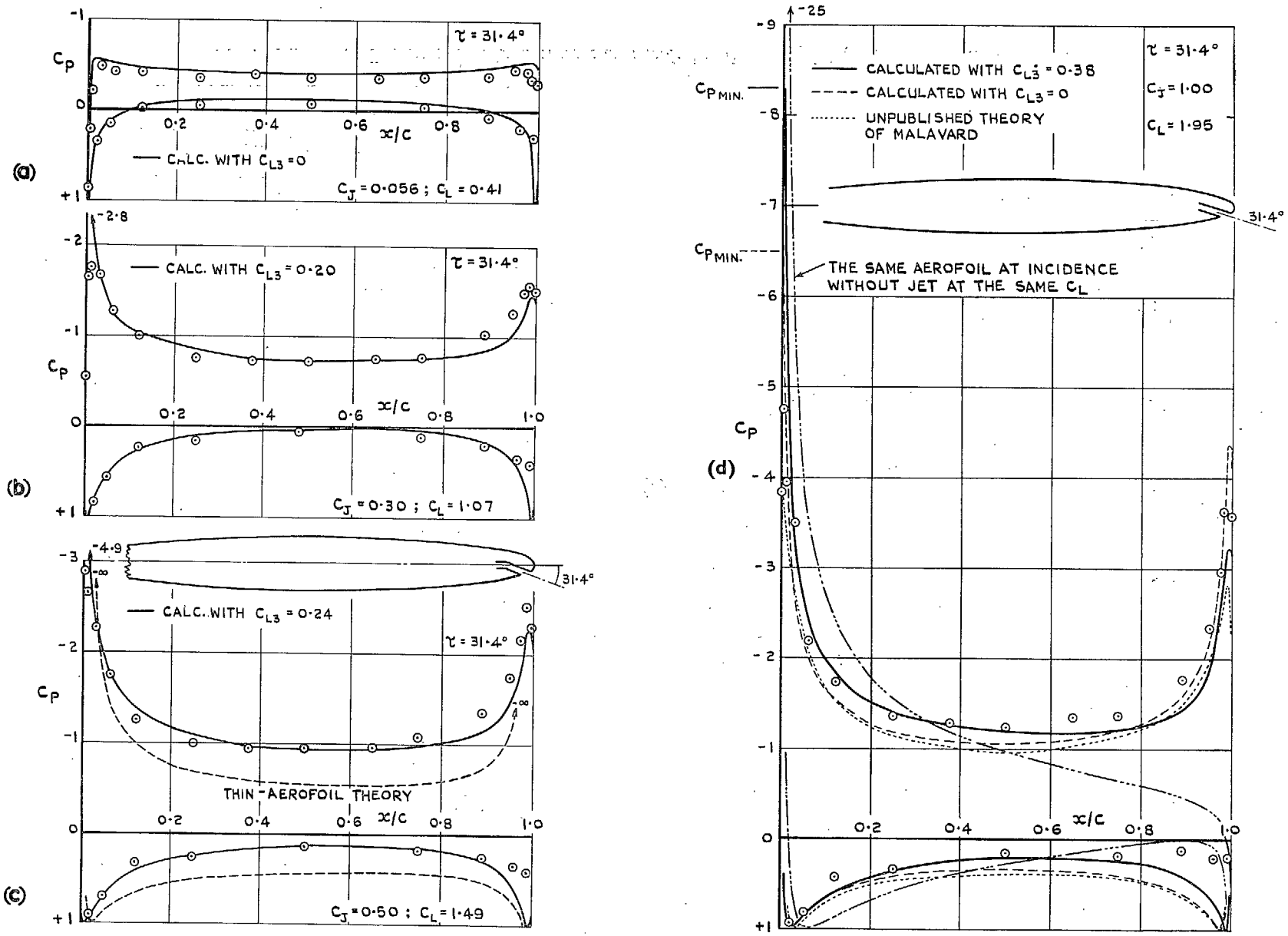

FIGS. 6a to 6d. Pressure distributions over an aerofoil with 30-deg jet (From Dimmock's tests[10]).

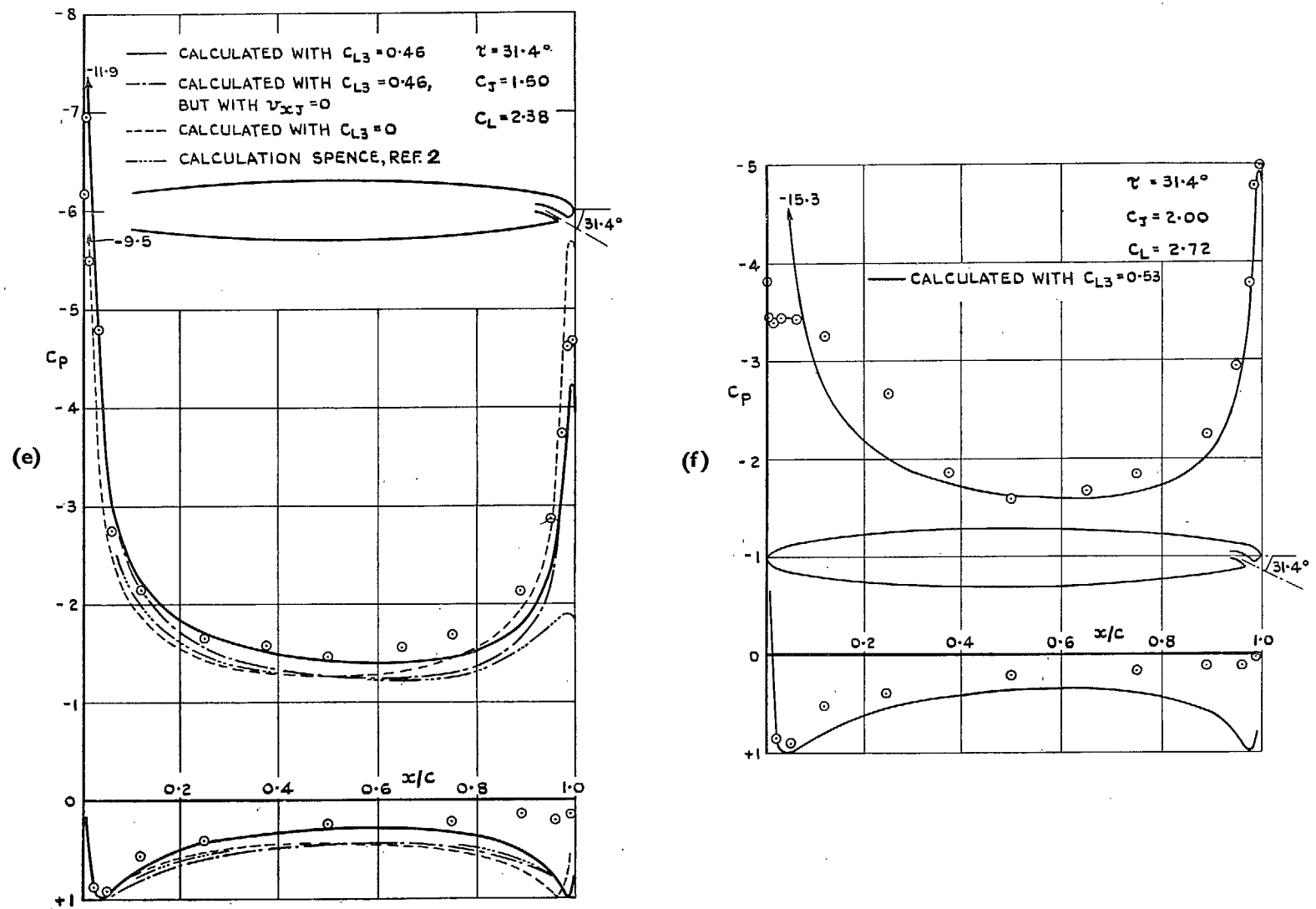

FIGS. 6e and 6f. Pressure distribution over an aerofoil with 30-deg jet (From Dimmock's tests[10]).

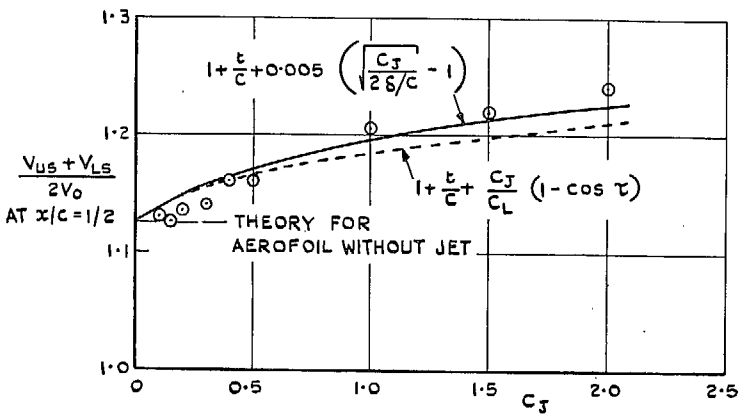

FIG. 7. Mean velocity on an aerofoil with 30-deg jet (From Dimmock's tests[10]).

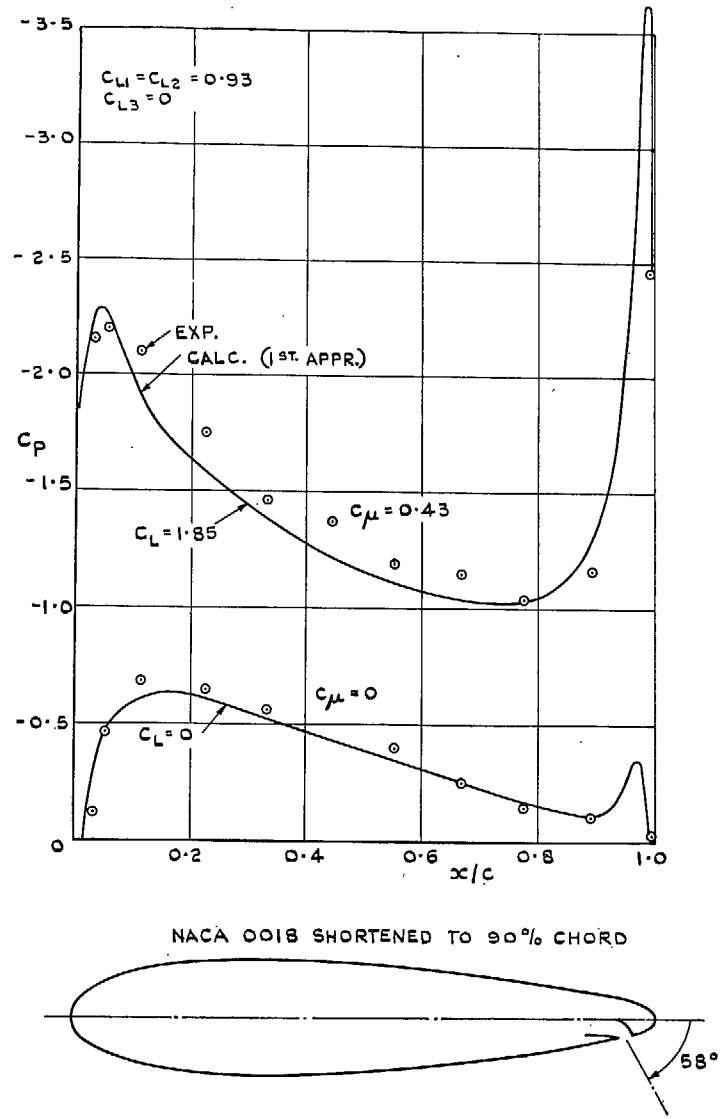

FIG. 8. Pressure distributions over an aerofoil with 58-deg jet (From O.N.E.R.A. Fiche Documentaire Provisoire 84. 29th August, 1955).

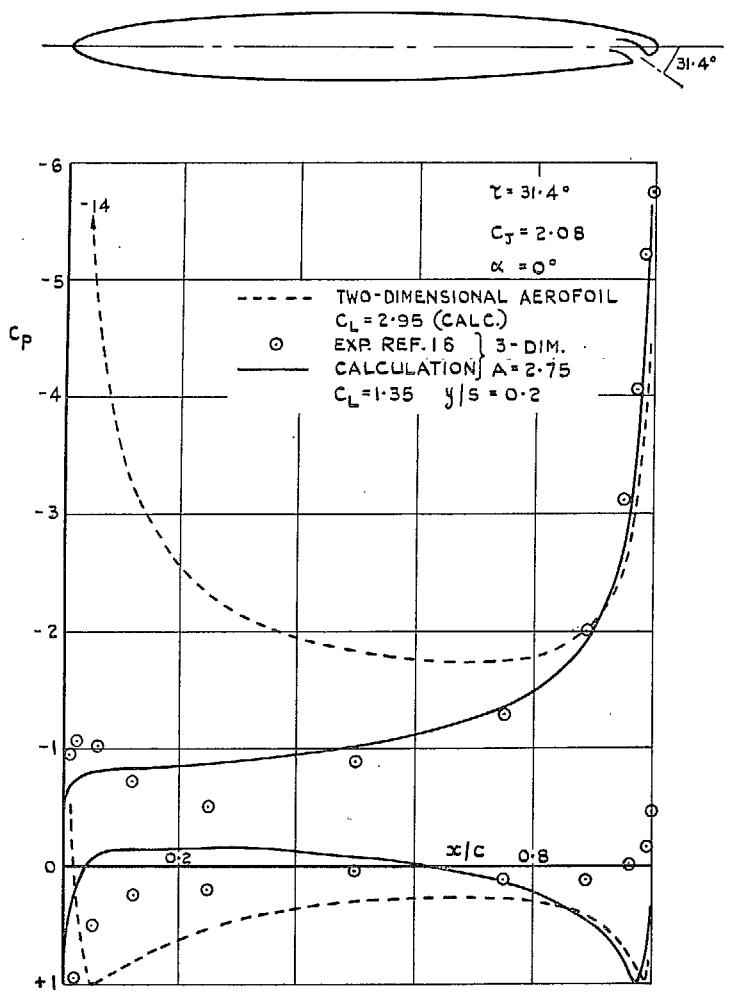

FIG. 9. Pressure distribution over a section of a three-dimensional wing from tests by Williams and Alexander[16].

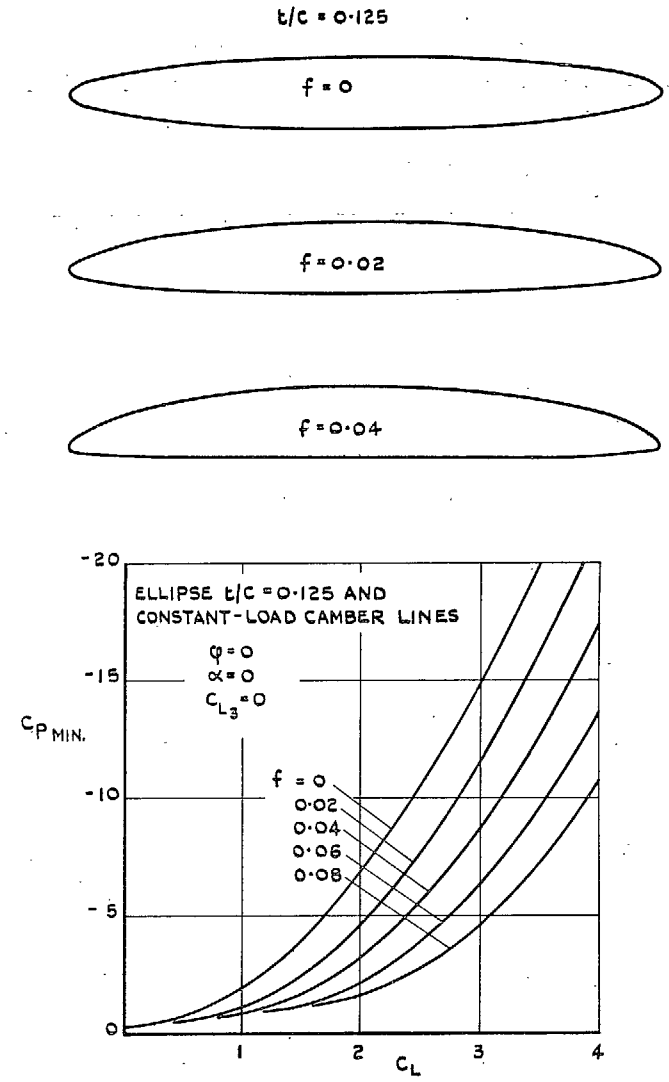

FIG. 10. Shapes and minimum pressure coefficients for some cambered aerofoils with constant-load camber-lines. $t/c = 0 \cdot 125$.

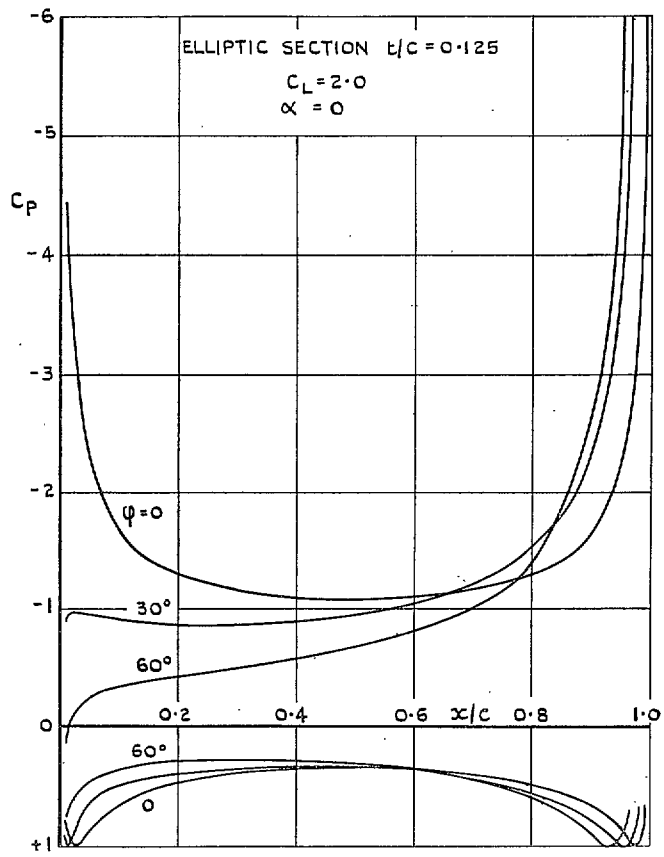

FIG. 11. Pressure distribution at the centre-section of an infinite swept-back wing with lift at zero incidence.

(68986) Wt. 20/9036 K7 11/57 Hw.

PRINTED IN GREAT BRITAIN

Publications of the Aeronautical Research Council

ANNUAL TECHNICAL REPORTS OF THE AERONAUTICAL RESEARCH COUNCIL (BOUND VOLUMES)

1939 Vol. I. Aerodynamics General, Performance, Airscrews, Engines. 50*s.* (51*s.* 9*d.*).
Vol. II. Stability and Control, Flutter and Vibration, Instruments, Structures, Seaplanes, etc. 63*s.* (64*s.* 9*d.*)

1940 Aero and Hydrodynamics, Aerofoils, Airscrews, Engines, Flutter, Icing, Stability and Control Structures, and a miscellaneous section. 50*s.* (51*s.* 9*d.*)

1941 Aero and Hydrodynamics, Aerofoils, Airscrews, Engines, Flutter, Stability and Control Structures. 63*s.* (64*s.* 9*d.*)

1942 Vol. I. Aero and Hydrodynamics, Aerofoils, Airscrews, Engines. 75*s.* (76*s.* 9*d.*)
Vol. II. Noise, Parachutes, Stability and Control, Structures, Vibration, Wind Tunnels. 47*s.* 6*d.* (49*s.* 3*d.*)

1943 Vol. I. Aerodynamics, Aerofoils, Airscrews. 80*s.* (81*s.* 9*d.*)
Vol. II. Engines, Flutter, Materials, Parachutes, Performance, Stability and Control, Structures. 90*s.* (92*s.* 6*d.*)

1944 Vol. I. Aero and Hydrodynamics, Aerofoils, Aircraft, Airscrews, Controls. 84*s.* (86*s.* 3*d.*)
Vol. II. Flutter and Vibration, Materials, Miscellaneous, Navigation, Parachutes, Performance, Plates and Panels, Stability, Structures, Test Equipment, Wind Tunnels. 84*s.* (86*s.* 3*d.*)

1945 Vol. I. Aero and Hydrodynamics, Aerofoils. 130*s.* (132*s.* 6*d.*)
Vol. II. Aircraft, Airscrews, Controls. 130*s.* (132*s.* 6*d.*)
Vol. III. Flutter and Vibration, Instruments, Miscellaneous, Parachutes, Plates and Panels, Propulsion. 130*s.* (132*s.* 3*d.*)
Vol. IV. Stability, Structures, Wind Tunnels, Wind Tunnel Technique. 130*s.* (132*s.* 3*d.*)

Annual Reports of the Aeronautical Research Council—

1937 2*s.* (2*s.* 2*d.*) 1938 1*s.* 6*d.* (1*s.* 8*d.*) 1939–48 3*s.* (3*s.* 3*d.*)

Index to all Reports and Memoranda published in the Annual Technical Reports, and separately—

April, 1950 - - - - R. & M. 2600 2*s.* 6*d.* (2*s.* 8*d.*)

Author Index to all Reports and Memoranda of the Aeronautical Research Council—

1909—January, 1954 R. & M. No. 2570 15*s.* (15*s.* 6*d.*)

Indexes to the Technical Reports of the Aeronautical Research Council—

December 1, 1936—June 30, 1939	R. & M. No. 1850	1*s.* 3*d.* (1*s.* 5*d.*)
July 1, 1939—June 30, 1945	R. & M. No. 1950	1*s.* (1*s.* 2*d.*)
July 1, 1945—June 30, 1946	R. & M. No. 2050	1*s.* (1*s.* 2*d.*)
July 1, 1946—December 31, 1946	R. & M. No. 2150	1*s.* 3*d.* (1*s.* 5*d.*)
January 1, 1947—June 30, 1947	R. & M. No. 2250	1*s.* 3*d.* (1*s.* 5*d.*)

Published Reports and Memoranda of the Aeronautical Research Council—

Between Nos. 2251–2349	R. & M. No. 2350	1*s.* 9*d.* (1*s.* 11*d.*)
Between Nos. 2351–2449	R. & M. No. 2450	2*s.* (2*s.* 2*d.*)
Between Nos. 2451–2549	R. & M. No. 2550	2*s.* 6*d.* (2*s.* 8*d.*)
Between Nos. 2551–2649	R. & M. No. 2650	2*s.* 6*d.* (2*s.* 8*d.*)

Prices in brackets include postage

HER MAJESTY'S STATIONERY OFFICE

York House, Kingsway, London, W.C.2; 423 Oxford Street, London, W.1; 13a Castle Street, Edinburgh 2; 39 King Street, Manchester 2; 2 Edmund Street, Birmingham 3; 109 St. Mary Street, Cardiff; Tower Lane, Bristol, 1; 80 Chichester Street, Belfast, *or through any bookseller.*

S.O. Code No. 23-3036